Quantum-Interference-Enhanced Phonon Laser in Cavity Optomechanics

Changyong Lei and Jie Ren*

Center for Phononics and Thermal Energy Science, China-EU Joint Lab on Nanophononics, Shanghai Key Laboratory of Special Artificial Microstructure Materials and Technology, School of Physics Science and Engineering, Tongji University, Shanghai 200092, China

(Received 14 March 2023; revised 26 April 2023; accepted 4 May 2023; published 31 May 2023)

Cavity-optomechanics-based phonon lasers are traditionally described in terms of three-mode resonance, while the energy nonconservation optomechanical terms are conventionally ignored. Here, we present a complete theory of phonon lasers, emphasizing the importance of the previously omitted optomechanical interaction. We show that this indispensable optomechanical interaction is equivalent to a Kerr nonlinear interaction. Analytical results show that the interference between this Kerr-type interaction and three-mode resonance adds a transition channel with no phonon emission or absorption, thus enhancing phonon lasing and realizing an ultralow-threshold phonon laser and even a phonon cooler. The interference effect produces an asymmetric gain profile with a Fano spectral shape in addition to the traditional Lorentzian shape. Our complete theory shows perfect agreement with existing experiments and provides a new degree of freedom to manipulate optomechanical phonon lasers.

DOI: 10.1103/PhysRevApplied.19.054093

I. INTRODUCTION

Phonon lasers, which are analogous to optical lasers, produce coherent amplification of mechanical oscillations, which is of great importance for high-precision sensing and imaging [1–3], precision metrology [4,5], gravitational-wave detection [6], quantum synchronization [7], anomalous cooling [8], integrated phonon-photon chips [9,10], quantum information [11], and nonclassical-state engineering [1]. Phonon lasers have been experimentally demonstrated in a wide range of physical systems, such as harmonically trapped ions [12], optical tweezers [1], active levitated optomechanical systems [13], cavity optomechanics [14–16], ultracold atoms [17], quantum dots [18,19], nanomechanical resonators [20,21], and superlattice structures [22].

Among the various realization schemes, the phonon laser [14] based on cavity optomechanics [23] (COM) has recently attracted increasing attention due to its flexibly controllable amplifying spectrum from the radio-frequency to the microwave regime, ultralow lasing threshold [15], and pronounced linewidth broadening [16]. The COM phonon laser consists of two optical cavities (acting as a two-level system) interacting with a mechanical breathing mode [14–16]. This kind of optical system has been widely used to realize optical memory [24], slow light [25,26], parity-time symmetry and optical isolation [27,28], optical nonreciprocity [29], electromagnetically induced transparency [30], quantum sensors [31], quantum networks [32,33], and phonon and photon amplification [34,35]. Based on this COM device, a variety of novel phonon lasers have been investigated, such as $\mathcal{PT}$-symmetric [36] and exceptional-point phonon lasers in non-Hermitian systems [16,37,38] and nonreciprocal phonon lasers in spinning resonators [39].

The previous theories [14,34,36,39,40] of this phonon laser are all described by a three-mode resonance, where the transition between optical supermodes accompanies a phonon emission or absorption, while the conventional optomechanical interaction (energy nonconservation terms) inducing virtual transitions is omitted by a rotating-wave approximation. These theories successfully interpret the experimental results [14,15], but only qualitatively, without accurate comparison. Therefore, a complete phonon-laser theory capable of quantitatively and accurately explaining the lasing experiments is highly desirable. Naturally, the neglected optomechanical terms [14,34,36,39,40] should be reconsidered for a reasonable complete theory of optomechanical phonon lasers.

The conventional optomechanical interaction can be recognized as equivalent to a Kerr nonlinear effect [41,42]. The nonlinear effect can induce a nonreciprocity of phonon transmission [43] to realize a phonon diode [44], and can also be used to generate quantum effects such as photon blockade [45–50] and phonon blockade [51–53]. With a weak Kerr nonlinearity, the unconventional photon blockade [54–57] is induced by the quantum interference

*Xonics@tongji.edu.cn

between multiple excitation paths. The quantum interference effect has thus been responsible for many novelties, such as electromagnetically induced transparency [58,59], lasing without inversion [60,61], Fano resonance [62,63], and virtual-real excitations interference [64]. However, the quantum interference in phonon lasing has not yet been explored.

In this paper, with re-emphasis on the importance of the omitted optomechanical interaction, which is equivalent to a Kerr-type interaction, the indispensable transition between optical supermodes without phonon emission or absorption is reconsidered in addition to the conventional phonon lasing channel. This transition is induced by interference between Kerr-type interaction and three-mode resonance, and depends on both the optomechanical coupling strength and the total photon number. The interference effect causes an asymmetric gain profile of Fano spectral shape. By tuning the optomechanical coupling strength, the phonon lasing can be significantly enhanced or, on the contrary, even turned to a phonon cooler.

The remainder of the paper is organized as follows. In Sec. II, we introduce the cavity optomechanical phonon-laser system and model. We discuss the essential physics of the Hamiltonian and emphasize that the Kerr-type interaction plays a very important role in a phonon laser. In Sec. III, we evaluate an analytical formula for the gain of a phonon laser. In Sec. IV, with the numerical results, we discuss the laser gain, and the threshold power for resonance and nonresonance cases. We show that, by tuning, the optomechanical coupling strength can realize a laser to cooler transformation. Finally, a summary is given in Sec. V.

II. SYSTEM AND MODEL

COM phonon lasers can be realized in various typical schemes, such as two coupled cavities interacting with a middle moveable mirror by radiation pressures [Fig. 1(a)], or two coupled whispering gallery cavities with one cavity coupled with a vibrational breathing mode [Fig. 1(b)]. In both schemes, one optical cavity is driven by a laser with frequency ω_L and amplitude $\eta = \sqrt{2\gamma_i P_{\text{in}}/(\hbar\omega_L)}$, where γ_i is the ith cavity's decay rate and P_{in} is the input power. Thereafter, we set $\hbar = 1$.

The interaction between two cavities and the mechanical oscillator can be generally expressed as (a complete Hamiltonian, see Appendix A) $\hat{V} = (\hat{b} + \hat{b}^\dagger)(g_1\hat{n}_1 + g_2\hat{n}_2)$, where $\hat{n}_i = \hat{a}_i^\dagger\hat{a}_i$ are the photon number operators, with $\hat{a}_i^\dagger$ ($\hat{a}_i$) and $\hat{b}^\dagger$ ($\hat{b}$) being the creation (annihilation) operators of the cavity field i and mechanical oscillator, respectively. The optomechanical coupling strength is $g_1 = -g_2$ for the first scheme [Fig. 1(a)] and $g_1 = 0$ for the second scheme [Fig. 1(b)]. In fact, in the first scheme, we can realize $|g_1| \neq |g_2|$ by choosing two cavities with the same resonant frequencies but filled with different media (different refractive indices) or different transverse electromagnetic modes.

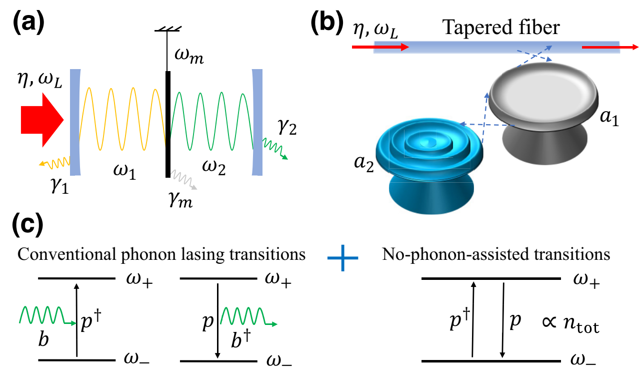

FIG. 1. Schematic illustration of phonon lasers. (a) A cavity optomechanics system composed of a moveable membrane placed inside an optical cavity, and the two optical modes coupled via transmission. (b) A conventional phonon laser composed by two coupled whispering gallery cavities, with one cavity supporting a mechanical breathing mode. (c) In the supermode picture, the phonon lasing channels are superposed by the conventional phonon lasing transitions channel and the no-phonon-assisted transition channels; see discussion after Eq. (2).

We can rewrite $\hat{V} = \hat{V}_d + \hat{V}_a$, where $\hat{V}_a = \lambda(\hat{b} + \hat{b}^\dagger)(\hat{n}_2 + \hat{n}_1)$ and $\hat{V}_d = g(\hat{b} + \hat{b}^\dagger)(\hat{n}_2 - \hat{n}_1)$, with coupling strengths $\lambda = (g_2 + g_1)/2$ and $g = (g_2 - g_1)/2$, respectively. Rewritten with supermode operators $\hat{a}_\pm = (\hat{a}_2 \pm \hat{a}_1)/\sqrt{2}$ and omitting the energy nonconservation terms, one can see that $\hat{V}_d = g(\hat{p}^\dagger\hat{b} + \hat{b}^\dagger\hat{p})$ (with $\hat{p} = \hat{a}_-^\dagger\hat{a}_+$ the polarization transition operator) is the conventional three-mode resonance interaction adopted to describe the phonon lasing Hamiltonian [14,34,36,39,40]. As such, the Hamiltonian of the COM phonon laser can be generally written as (with a frame rotating at frequency ω_L)

$$\hat{H} = \omega_m\hat{b}^\dagger\hat{b} + \omega_+\hat{n}_+ + \omega_-\hat{n}_- + \hat{H}_{\text{drive}} + g(\hat{p}^\dagger\hat{b} + \hat{b}^\dagger\hat{p}) + \lambda(\hat{b} + \hat{b}^\dagger)\hat{n}_{\text{tot}}, \tag{1}$$

with the driving term $\hat{H}_{\text{drive}} = \eta(\hat{a}_+^\dagger - \hat{a}_-^\dagger)/\sqrt{2} + \text{h.c.}$, ω_m being the phonon frequency, and $\omega_\pm$ being the frequencies of up and down supermodes $\hat{n}_\pm = \hat{a}_\pm^\dagger\hat{a}_\pm$, respectively. It is crucial to notice that the last term, the optomechanical interaction $\hat{V}_a = \lambda(\hat{b} + \hat{b}^\dagger)\hat{n}_{\text{tot}}$ ($\hat{n}_{\text{tot}} = \hat{n}_+ + \hat{n}_- = \hat{n}_1 + \hat{n}_2$), has always been omitted in previous phonon-laser theory as a convention [14,34,36,39,40].

However, as we will demonstrate, this traditionally disregarded term plays an important role in the COM phonon laser. This can be seen by the unitary transformation $\tilde{H} =$

$\hat{U}^\dagger \hat{H} \hat{U}$ with $\hat{U} = e^{-(\lambda/\omega_m)(\hat{b}^\dagger - \hat{b})\hat{n}_{\text{tot}}}$, so that

$$\tilde{H} = \omega_m \hat{b}^\dagger \hat{b} + \omega_+ \hat{n}_+ + \omega_- \hat{n}_- + \tilde{H}_{\text{dr}} + g(\hat{p}^\dagger \hat{b} + \hat{b}^\dagger \hat{p}) - (\lambda g/\omega_m)(\hat{p}^\dagger + \hat{p})\hat{n}_{\text{tot}} - (\lambda^2/\omega_m)\hat{n}_{\text{tot}}^2, \tag{2}$$

where $\tilde{H}_{\text{drive}} = \hat{U}^\dagger \hat{H}_{\text{drive}} \hat{U}$ is the driving term (see Appendix A). The last term in Eq. (2), coming from $U^\dagger \hat{V}_d U$, is a Kerr-type nonlinear effect, which renormalizes the supermode levels.

More interestingly, the second-to-last term $(\lambda g/\omega_m)(\hat{p}^\dagger + \hat{p})\hat{n}_{\text{tot}}$ denotes the interference of the three-mode resonance (with strength g) and the Kerr-type interaction (with strength λ). This interference term causes an additional transition [Fig. 1(c)] from the up (down) supermode to down (up) supermode without phonon emission (absorption). This is different from the conventional phonon lasing composed by a three-mode resonance, where transitions are associated with a phonon emitting or absorbing. The interference-induced no-phonon-assisted photon transition processes [Fig. 1(c)] will have a significant impact on the up-down optical supermodes so as to influence the phonon emission or absorption, especially at large photon number, $\hat{n}_{\text{tot}} \sim \omega_m/\lambda$ (Refs. [39,65] show $\hat{n}_{\text{tot}} \approx 10^5$–$10^7$). Moreover, in the original optical mode picture, $(\hat{p}^\dagger + \hat{p})\hat{n}_{\text{tot}} = \hat{n}_2^2 - \hat{n}_1^2$, which indicates that the interference effect in the supermode picture corresponds to the difference of Kerr nonlinearities of cavities 1 and 2. The Kerr-type nonlinearity is not intrinsic to the photon cavities, but is induced by the coherent phonon $\hat{b}^\dagger + (\lambda/\omega_m)\hat{n}_{\text{tot}}$, dressed by photons.

III. ANALYTIC RESULTS OF PHONON LASER

We define the population-inversion operator as $\Delta\hat{n} = \hat{n}_+ - \hat{n}_-$ and the optical energy difference $\omega_p = \omega_+ - \omega_-$. The equations of motion of the phonon lasing system are given by

$$\begin{aligned}
\frac{d\hat{a}_+}{dt} &= -(i\omega_+ + \gamma)\,\hat{a}_+ - i\lambda\left(\hat{b} + \hat{b}^\dagger\right)\hat{a}_+ - ig\hat{a}_-\hat{b} - i\frac{\eta}{\sqrt{2}}, \\
\frac{d\hat{a}_-}{dt} &= -(i\omega_- + \gamma)\,\hat{a}_- - i\lambda\left(\hat{b} + \hat{b}^\dagger\right)\hat{a}_- - ig\hat{a}_+\hat{b}^\dagger + i\frac{\eta}{\sqrt{2}}, \\
\frac{d\hat{p}}{dt} &= -\left(i\omega_p + 2\gamma\right)\hat{p} + ig\Delta\hat{n}\hat{b} - i\frac{\eta}{\sqrt{2}}\left(\hat{a}_+ + \hat{a}_-^\dagger\right), \\
\frac{d\hat{b}}{dt} &= -(i\omega_m + \gamma_m)\,\hat{b} - i\lambda\hat{n}_{\text{tot}} - ig\hat{p},
\end{aligned} \tag{3}$$

with $\gamma = (\gamma_1 + \gamma_2)/2$ being the average decay rate of two optical cavities and γ_m being the phonon decay rate of the mechanical breathing mode. Clearly, the non-negligible terms with nonzero λ have a significant impact on the equations of motion.

To find the phonon lasing gain, we solve these equations in the weak coupling regime with $\gamma_m \ll \gamma$. With the slowly varying amplitudes $\hat{b} = \tilde{b}e^{-i\omega_m t}$ and $\hat{p} = \tilde{p}e^{-i\omega_m t}$, and the standard procedures (see Appendix B for more details), we obtain the lasing gain G as $d\tilde{b}/dt = \left(G - \gamma_m - i\omega'\right)\tilde{b}$. The coherent amplification of stimulated emitted phonons will emerge once $G \gg \gamma_m$. Keeping up to the second orders of g and η, we can finally obtain the phonon-laser gain as $G = G_0 + G_1 + G_2$, where

$$G_0 = \frac{\gamma g^2 \Delta\hat{n}}{2\left(\omega_p - \omega_m\right)^2 + 8\gamma^2}, \tag{4}$$

$$G_1 = \frac{\lambda}{g}\left[1 - \frac{2\omega_p}{\omega_m} f\left(-\frac{\gamma}{\omega_p}\right)\right] G_0, \tag{5}$$

$$G_2 = \frac{2\lambda}{g}\frac{\omega_p - \omega_m}{\omega_m} f\left(\frac{\omega_p}{4\gamma}\right) G_0, \tag{6}$$

with the Fano-like spectrum profile

$$f(x) = \frac{(x + \Omega)^2}{1 + \Omega^2} - \frac{x^2}{1 + \Omega^2}, \tag{7}$$

where $\Delta\hat{n} = -4\Delta_L\omega_m\eta^2 / \left[\gamma^2\omega_p^2\left(1 + \Omega^2\right)\right]$ denotes photon-number inversion, and $\Omega = \left[\Delta_L^2 - \left(\omega_p/2\right)^2 + \gamma^2\right] \Big/ \left(\gamma\omega_p\right)$. Here $\Delta_L = \omega_c - \omega_L$ is the detuning between the optical cavities ω_c and the drive laser frequency; and x denotes the Fano parameter.

Clearly, here G_0 is the conventional phonon-laser gain of symmetric Lorentz spectrum shape, generated merely by the three-mode resonance [39], while G_1 and G_2 are the additional gains induced with the indispensable Kerr-type interaction manifested by the nonzero λ, which are ignored in previous literature [14,36,39,40]. At resonant condition $\omega_p = \omega_m$, G_1 is finite but G_2 vanishes, i.e., G_2 is caused by the nonresonance excitation ($\omega_p \neq \omega_m$). The terms G_1 and G_2 contain both the three-mode resonance strength g and the Kerr-type interaction coupling strength λ, and the contained spectrum profile $f(x)$ is superposed by Fano-type [the first term in Eq. (7)] and Lorentz-type [the second term in Eq. (7)] shapes, which indicates that G_1 and G_2 are induced by an interference effect.

IV. NUMERICAL RESULTS AND DISCUSSION

First, we consider the resonance excitation ($\omega_p = \omega_m$) case, i.e., $G_2 = 0$. Figure 2(a) shows the phonon gain as functions of detuning Δ_L and the optomechanical coupling strength ratio λ/g, with parameters I [14,39]. Because $\lambda = (g_2 + g_1)/2$ and $g = (g_2 - g_1)/2$, where g_1 and g_2 are the optomechanical coupling strengths of cavities 1 and 2, respectively, we can transform λ/g from >0 to <0 by tuning g_1 and g_2. This can be realized in both schemes we have listed in Figs. 1(a) and 1(b). In the first case [Fig. 1(a)], due to g_1 and g_2 having opposite signs (suppose $g_1 < 0$ and $g_2 > 0$, i.e., $g > 0$), by tuning g_1 and g_2 (filled with different media), we can change from $|g_1| > |g_2|$ to $|g_1| < |g_2|$, i.e., change from $\lambda < 0$ ($\lambda/g < 0$) to $\lambda > 0$ ($\lambda/g > 0$). In the second case [Fig. 1(b)], due to both $g_1, g_2 > 0$ ($\lambda > 0$), we can adjust g_1 and g_2 to realize the change from $g_1 < g_2$ to $g_1 > g_2$, i.e., the change from $g < 0$ ($\lambda/g < 0$) to $g > 0$ ($\lambda/g > 0$). By tuning λ/g, the no-phonon-assisted transition can enhance the phonon lasing process compared with the case of G_0 at $\lambda = 0$ (this corresponds to the conventional phonon-laser theory disregarding the energy nonconservation optomechanical terms [14,34,36,39,40]).

We note that, if we merely consider G_0 as in previous experiments [14], the gain peak of $G_0 \approx 0.5\gamma_m$ [$\lambda/g = 0$, the green line in Fig. 2(a)] is less than the loss γ_m, i.e., there is no phonon laser generated, in contradiction with the experimental results [14]. This contradiction can be well solved by considering the indispensable Kerr-type interaction, where we see the complete phonon gain $G = G_0 + G_1 > \gamma_m$ [the red line in Fig. 2(a) with $\lambda/g = 1$], which is consistent with the experimental results [14]. Because $\gamma \ll \omega_p$, $\gamma/\omega_p \to 0$, and then $G_1 = (\lambda/g)[(1-\Omega^2)/(1+\Omega^2)]G_0$ means that the total phonon gain G at positive λ has a symmetric Lorentz resonance profile with a narrower linewidth than the conventional phonon gain G_0 at $\lambda = 0$. Moreover, the transformation from a phonon laser ($G > \gamma_m$) to a phonon cooler ($G < 0$) [14,66–69] can be significantly realized at negative λ/g. Similar results are obtained for parameters II [15], which are not shown here for brevity.

Figure 2(b) shows the threshold input power of a phonon laser as a function of coupling strength λ. The threshold power is obtained as

$$P_{\text{th}} = P_{\text{th},0}\frac{G_0}{G}, \quad \text{where}$$
$$P_{\text{th},0} = C_{\Delta_L}\left(1+\Omega^2\right)\left[\left(\omega_p - \omega_m\right)^2 + 4\gamma^2\right]/g^2, \tag{8}$$

is the conventional laser threshold power (without Kerr nonlinear effect) given by $G_0 = \gamma_m$, where $C_{\Delta_L} = -\hbar\gamma\gamma_m\omega_L\omega_p^2/(4\gamma_1\omega_m\Delta_L)$ [39]. We see in both parameter sets I and II that, with increasing λ, the threshold powers P_{th} are significantly reduced, since $G > G_0$.

From Eqs. (4), (5), and (8), we get $G_0/G \propto (1+\lambda/g)^{-1}$ and $P_{\text{th},0} \propto g^{-2}$, so that, for $\lambda \ll g$, the threshold power $P_{\text{th}} \propto g^{-2}$; while, when $\lambda \gg g$, then $P_{\text{th}} \propto g^{-1}$ and λ^{-1}. This indicates that, by increasing g and λ, ultralow-threshold phonon lasing can be realized. When only one optical cavity is optomechanically coupled with the vibrational mode, as in the experimental schemes of Refs. [14,15], i.e., $g_1 = 0$ as shown in Fig. 1(b)), we have $\lambda/g = 1$ and obtain the threshold powers as 6.3 μW [blue star in Fig. 2(b)] for parameters I and 1.2 μW [red star in Fig. 2(b)] for parameters II, respectively.

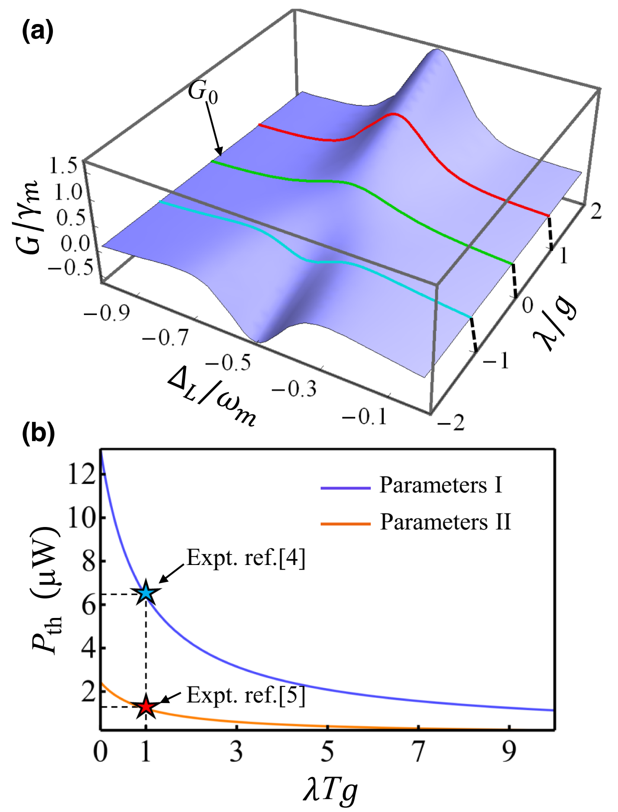

FIG. 2. Phonon lasing at the resonance case $\omega_p = \omega_m$. (a) The phonon gain G as functions of Δ_L and coupling strength λ. Three typical laser gain profiles $G > \gamma_m$, $G = G_0$ (the convention phonon gain), and $G < 0$ are depicted, for $\lambda/g = 1$ (red line), 0 (green line), and −1 (cyan line), respectively. Here the parameters I and input power 7 μW are used. (b) The threshold powers of phonon laser as a function of λ; blue line for parameters I and orange line for parameters II. Vahala's [14] (the dark blue star) and Xiao's [15] (the red star) experimental results are marked. Parameters I [14,39]: the vibration frequency is $\omega_m = 2\pi \times 23.4$ MHz; the quality factors of optical cavities and mechanical oscillator are $Q_1 = 3 \times 10^7$, $Q_2 = 9.7 \times 10^7$, and $Q_m = 625$, respectively; the decay rates are given by $\gamma_{1,2} = \omega_c/Q_{1,2}$ and $\gamma_m = \omega_m/Q_m$; the diameters of the optical cavities are $R = 69$ μm; the optomechanical coupling strength is $g = (\omega_c/R)\sqrt{(\hbar/2m\omega_m)}$. Parameters II [15]: $\omega_m = 2\pi \times 59.2$ MHz; $Q_1 = 2.5 \times 10^7$, $Q_2 = 9.7 \times 10^7$, and $Q_m = 18\,000$; and $R = 60$ μm. A 1550 nm driving laser and 50 ng mechanical oscillator are used for Parameters I and II.

As one can see, the analytical theory results are consistent with Vahala's [14] and Xiao's [15] experimental results, respectively. But, for the conventional phonon-laser theory without three-mode resonance and Kerr interaction interference ($\lambda = 0$), the threshold power is almost twice as large as the experimental results [see the threshold powers at $\lambda = 0$ in Fig. 2(b)]. These results demonstrate that the interference effect is indispensable for a reasonable complete phonon-laser theory that accurately explains experiments.

Second, we explore the nonresonance excitation case ($\omega_p \neq \omega_m$). Figure 3(a) depicts the phonon gain profiles at the nonresonance condition with $\omega_p = 1.4\omega_m$, which indeed have asymmetric Fano shapes. The components of laser gain G_1 and G_2 induced by the interference effect are much larger than the conventional laser gain G_0, and especially G_2 dominates at this nonresonance condition. Gain G_2 is almost antisymmetric about the axis $\Delta_L = -\omega_p/2$, while G_1 approaches a symmetric shape, so that the joint effect of G_1 and G_2 causes laser gain G to have an asymmetric Fano shape. Figure 3(a) also shows that, with the detuning Δ_L in the range $(-0.8\omega_m, -0.7\omega_m)$, a phonon laser ($G > \gamma_m$) is generated, but in the region $\Delta_L > -0.68\omega_m$ there is a phonon cooler ($G < 0$).

Figure 3(b) shows that the amplitudes of gain are increased with increasing optomechanical coupling strength λ, i.e., the laser gains are increased in the region $\Delta_L \in (-0.8\omega_m, -0.7\omega_m)$, while the cooling effects are increased for $\Delta_L > -0.68\omega_m$. Figure 3(c) shows that, with increasing difference of $|\omega_p - \omega_m|$, i.e., further away from the resonance condition, the laser gains are decreased. Moreover, the gain shapes for $\pm|\omega_p - \omega_m|$ are asymmetric about the resonance excitation ($\omega_p = \omega_m$). By using Eq. (8), we can calculate the laser threshold power for nonresonance excitation. Figure 3(d) shows that, far away from the resonance condition (increasing ω_p), the laser threshold powers are increased, but with increasing coupling strength λ, the laser threshold powers can be decreased, so that, by adjusting the Kerr-type interaction coupling strength λ, we can realize a phonon laser (cooler) with very low threshold power in the nonresonance case.

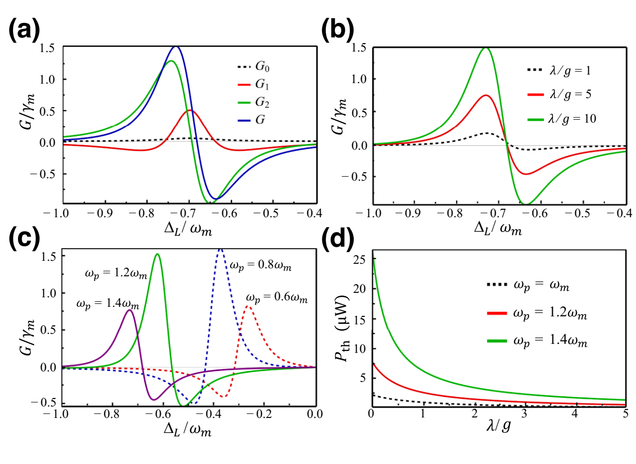

FIG. 3. Phonon lasing at the nonresonance case $\omega_p \neq \omega_m$. (a) The phonon-laser gain and its components with $\lambda/g = 10$ and $\omega_p = 1.4\omega_m$ as a function of detuning Δ_L are shown. (b),(c) Phonon-laser gains for different coupling strengths λ (with $\omega_p = 1.4\omega_m$) and optical energy differences ω_p (with $\lambda/g = 5$) are shown in (b) and (c), respectively. (d) The laser threshold powers for different ω_p and λ are shown. Here, the other parameters are given by parameters II.

In both the resonance and nonresonance cases, the phonon lasing behavior can be significantly altered by tuning the optomechanical coupling strength λ. Thus, it provides a new freedom to manipulate this optomechanical system; for example, we can realize a phonon cooler by tuning the coupling strength λ in the resonance case [Fig. 2(a)], which can be helpful to realize the quantum ground state of a mechanical oscillator [70–72] and the entanglement of macroscopic vibrators [73,74]. In the nonresonance case, with the Fano shape gain [Fig. 3(a)], it is very sensitive to the detuning (i.e., a very small change in detuning turns the phonon laser into a phonon cooler), so it can be used to realize a highly sensitive sensor [75–77].

Quantum interference plays a very important role in our phonon-laser theory. Here, we emphasize that "quantum" originated from the energy nonconservation transition which is caused by the interference effect between the Kerr-type interaction and three-mode resonance. This differs from a recent experiment [78] in which a Paul trap was used to co-trap two ion species to realize a phonon laser in the quantum regime. In their work, "quantum" means that the phonon laser was operated close to the quantum ground state with an average phonon number <10. The phonon number statistics and correlation beyond this work will be discussed in the future.

V. SUMMARY

By reconsidering the Kerr-type optomechanical interaction, which was previously overlooked in traditional phonon-laser theory, we have obtained a reasonably complete theory for cavity-optomechanics-based phonon lasers, which precisely explains the existing experiments. With this indispensable optomechanical interaction, an additional transition without phonon assistance has been induced to the conventional phonon lasing channel, resulting in a phonon gain profile of asymmetric Fano shape. Thus, optomechanical phonon lasers can be enhanced with an ultralow threshold, or even a phonon cooler can be realized, by the transition without phonons. We hope that this complete theory could pave the way for quantitatively exploring further experiments of ultralow-threshold phonon lasers [15] and nonreciprocal phonon lasers [39]. Our work provides a new route to manipulate phonon lasers, and in the future may facilitate applications in high-precision imaging [79–81], ultrasensitive sensors and detection of ultraweak forces [75–77], steering phonon chips [13], high-frequency modulation [82], modulating a material's optical or electronic properties [18], nonclassical correlations of optomechanical systems [83], information processing [1], mechanical oscillator cooling [71,72], and macroscopic entanglement [73,74].

ACKNOWLEDGMENTS

This work is supported by the National Natural Science Foundation of China (Grant No. 11935010), the Natural Science Foundation of Shanghai (Grant Nos. 23ZR1481200, 23XD1423800), the National Key R&D Program of China (Grant No. 2022YFA1404400), and the Opening Project of Shanghai Key Laboratory of Special Artificial Microstructure Materials and Technology.

APPENDIX A: DERIVATION OF THE HAMILTONIAN

A general COM system is composed of two optical cavity modes ($\hat{a}_1$ and $\hat{a}_2$) coupled with a mechanical mode ($\hat{b}$) with coupling strengths g_1 and g_2, respectively (Fig. 1). We assume two optical cavities with the same resonant frequencies ω_c, and the mechanical mode with frequency ω_m and effective mass m. One of the optical cavities ($\hat{a}_1$) is driven by a laser with frequency ω_L and amplitude η. In this system, the couplings between optical modes and the mechanical mode are optomechanical interactions (radiation pressure), while the two optical modes are coupled by photon-hopping interaction with coupling strength J. The total Hamiltonian with a frame rotating at frequency ω_L is

$$\begin{aligned}\hat{H} = \omega_m \hat{b}^\dagger \hat{b} + \Delta_L \left(\hat{a}_1^\dagger \hat{a}_1 + \hat{a}_2^\dagger \hat{a}_2\right) + J\left(\hat{a}_1^\dagger \hat{a}_2 + \hat{a}_2^\dagger \hat{a}_1\right) \\ + \left(\hat{b} + \hat{b}^\dagger\right)\left(g_1 \hat{a}_1^\dagger \hat{a}_1 + g_2 \hat{a}_2^\dagger \hat{a}_2\right) + \eta\left(\hat{a}_1^\dagger + \hat{a}_1\right),\end{aligned} \tag{A1}$$

where $\Delta_L = \omega_c - \omega_L$.

The optomechanical interactions can be divided into two parts,

$$\begin{aligned}V &= g_1\left(\hat{b} + \hat{b}^\dagger\right)\hat{a}_1^\dagger \hat{a}_1 + g_2\left(\hat{b} + \hat{b}^\dagger\right)\hat{a}_2^\dagger \hat{a}_2 = \hat{V}_a + \hat{V}_d \\ &= \lambda(\hat{b} + \hat{b}^\dagger)(\hat{n}_2 + \hat{n}_1) + g(\hat{b} + \hat{b}^\dagger)(\hat{n}_2 - \hat{n}_1),\end{aligned} \tag{A2}$$

where $\lambda = (g_2 + g_1)/2$ and $g = (g_2 - g_1)/2$, and $\hat{n}_{1(2)} = \hat{a}_{1(2)}^\dagger \hat{a}_{1(2)}$. By using the supermode operators $\hat{a}_\pm = (\hat{a}_2 \pm \hat{a}_1)/\sqrt{2}$, we rewrite this Hamiltonian as

$$\hat{H} = \omega_m \hat{b}^\dagger \hat{b} + \omega_+ \hat{a}_+^\dagger \hat{a}_+ + \omega_- \hat{a}_-^\dagger \hat{a}_- + \hat{V}_a + \hat{V}_d + \hat{H}_{\text{drive}}, \tag{A3}$$

where the driving term is

$$\hat{H}_{\text{drive}} = \frac{\eta}{\sqrt{2}}\left(\hat{a}_+^\dagger - \hat{a}_-^\dagger + \hat{a}_+ - \hat{a}_-\right), \tag{A4}$$

and optomechanical terms are

$$\hat{V}_a = \lambda\left(\hat{b} + \hat{b}^\dagger\right)\left(\hat{a}_+^\dagger \hat{a}_+ + \hat{a}_-^\dagger \hat{a}_-\right), \tag{A5}$$

$$\hat{V}_d = g\left(\hat{b} + \hat{b}^\dagger\right)\left(\hat{a}_-^\dagger \hat{a}_+ + \hat{a}_+^\dagger \hat{a}_-\right), \tag{A6}$$

and $\omega_\pm = \Delta_L \pm J$. If we keep only the energy conservation terms in $\hat{V}_d$, then we get

$$\hat{V}_d = g\left(\hat{a}_+^\dagger \hat{a}_- \hat{b} + \hat{b}^\dagger \hat{a}_-^\dagger \hat{a}_+\right). \tag{A7}$$

Here $\hat{V}_d$ is the three-mode resonance term, which is used to generate the laser in the conventional phonon-laser theory [14,34,36,39,40], while $\hat{V}_a$ is the conventional optomechanical interaction, which is omitted in the conventional phonon-laser theory [14,34,36,39,40]. In what follows, we show that $\hat{V}_a$ is equivalent to an optical Kerr nonlinear effect, which is indispensable for a complete phonon-laser theory.

With the unitary operator $\hat{U} = e^{-(\lambda/\omega_m)(\hat{b}^\dagger - \hat{b})\hat{n}_{\text{tot}}}$, where $\hat{n}_{\text{tot}} = \hat{a}_+^\dagger \hat{a}_+ + \hat{a}_-^\dagger \hat{a}_-$ is the total particle number operator, we take the unitary transformation $\tilde{H} = \hat{U}^\dagger \hat{H} \hat{U}$ for the Hamiltonian given by Eq. (A3) with $\hat{V}_a$ and $\hat{V}_d$ given by (A5) and (A7), respectively. Then we get [Eq. (2) in the main text]

$$\begin{aligned}\tilde{H} = \omega_m \hat{b}^\dagger \hat{b} + \omega_+ \hat{n}_+ + \omega_- \hat{n}_- + \tilde{H}_{\text{drive}} + g\left(\hat{p}^\dagger \hat{b} + \hat{b}^\dagger \hat{p}\right) \\ - \frac{\lambda g}{\omega_m}(\hat{p}^\dagger + \hat{p})\hat{n}_{\text{tot}} - \frac{\lambda^2}{\omega_m}\hat{n}_{\text{tot}}^2,\end{aligned} \tag{A8}$$

where the driving term is

$$\begin{aligned}\tilde{H}_{\text{drive}} = \frac{\eta}{\sqrt{2}}\Big[\left(\hat{a}_+^\dagger - \hat{a}_-^\dagger\right) e^{(\lambda/\omega_m)\left(\hat{b}^\dagger - \hat{b}\right)} \\ + \left(\hat{a}_+ - \hat{a}_-\right) e^{-(\lambda/\omega_m)\left(\hat{b}^\dagger - \hat{b}\right)}\Big],\end{aligned} \tag{A9}$$

and $\hat{p} = \hat{a}_-^\dagger \hat{a}_+$ is the polarization transition operator. The last term of Eq. (A8) is an optical Kerr-type interaction, and the second-to-last term is the interference effect of three-mode resonance and Kerr interaction.

APPENDIX B: DERIVATION OF THE MECHANICAL GAIN

In order to derive the mechanical gain of the phonon laser, we begin with the Hamiltonian of Eq. (1) in the main text. With this Hamiltonian, the equations of motion for optical modes $\hat{a}_\pm$, polarization transition operator $\hat{p}$

($= \hat{a}_-^\dagger \hat{a}_+$), and phonon mode $\hat{b}$ are

$$\begin{aligned}
\frac{d\hat{a}_+}{dt} &= -\left(i\omega_+ + \gamma\right)\hat{a}_+ - i\lambda\left(\hat{b} + \hat{b}^\dagger\right)\hat{a}_+ \\
&\quad - ig\hat{a}_-\hat{b} - i\frac{\eta}{\sqrt{2}}, \\
\frac{d\hat{a}_-}{dt} &= -\left(i\omega_- + \gamma\right)\hat{a}_- - i\lambda\left(\hat{b} + \hat{b}^\dagger\right)\hat{a}_- \\
&\quad - ig\hat{a}_+\hat{b}^\dagger + i\frac{\eta}{\sqrt{2}}, \\
\frac{d\hat{p}}{dt} &= -\left(i\omega_p + 2\gamma\right)\hat{p} + ig\Delta\hat{n}\hat{b} - i\frac{\eta}{\sqrt{2}}\left(\hat{a}_+ + \hat{a}_-^\dagger\right), \\
\frac{d\hat{b}}{dt} &= -\left(i\omega_m + \gamma_m\right)\hat{b} - i\lambda\hat{n}_{\rm tot} - ig\hat{p}. \qquad \text{(B1)}
\end{aligned}$$

Here $\Delta\hat{n} = \hat{n}_+ - \hat{n}_-$ is the photon number inversion operator, $\hat{n}_{\rm tot} = \hat{a}_+^\dagger\hat{a}_+ + \hat{a}_-^\dagger\hat{a}_-$ is the total particle number operator, $\omega_p = \omega_+ - \omega_-$, and $\gamma = (\gamma_1 + \gamma_2)/2$. The equations of motion for the conjugate quantities, $\hat{a}_\pm^\dagger$, $\hat{p}^\dagger$, and $\hat{b}^\dagger$ can also be obtained just by using the conjugate transform for Eq. (B1) (not shown here).

We set $\hat{b} = \tilde{b}e^{-i\omega_m t}$ and $\hat{p} = \tilde{p}e^{-i\omega_m t}$; then we get

$$\begin{aligned}
\frac{d\hat{a}_+}{dt} &= -\left(i\omega_+ + \gamma\right)\hat{a}_+ - ig\hat{a}_-\tilde{b}e^{-i\omega_m t} \\
&\quad - i\lambda\left(\tilde{b}e^{-i\omega_m t} + \tilde{b}^\dagger e^{i\omega_m t}\right)\hat{a}_+ - i\frac{\eta}{\sqrt{2}}, \qquad \text{(B2)} \\
\frac{d\hat{a}_-}{dt} &= -\left(i\omega_- + \gamma\right)\hat{a}_- - ig\hat{a}_+\tilde{b}^\dagger e^{i\omega_m t} \\
&\quad - i\lambda\left(\tilde{b}e^{-i\omega_m t} + \tilde{b}^\dagger e^{i\omega_m t}\right)\hat{a}_- + i\frac{\eta}{\sqrt{2}}, \qquad \text{(B3)} \\
\frac{d\tilde{p}}{dt} &= -\left[i\left(\omega_p - \omega_m\right) + 2\gamma\right]\tilde{p} + ig\Delta\hat{n}\tilde{b} \\
&\quad - i\frac{\eta}{\sqrt{2}}\left(\hat{a}_+ + \hat{a}_-^\dagger\right)e^{i\omega_m t}, \qquad \text{(B4)} \\
\frac{d\tilde{b}}{dt} &= -\gamma_m\tilde{b} - i\lambda\hat{n}_{\rm tot}e^{i\omega_m t} - ig\tilde{p}. \qquad \text{(B5)}
\end{aligned}$$

With $\gamma \gg \gamma_m$, assuming the fields $\hat{a}_\pm$ and $\tilde{p}$ at steady state, by setting the time derivatives of $\hat{a}_\pm$ and $\tilde{p}$ to zero, and keeping λ and g to first order and η to second order in the total particle number operator $\hat{n}_{\rm tot}$ and polarization transition operator $\tilde{p}$, then we get

$$\hat{n}_{\rm tot} \approx \frac{g\eta^2}{2}\left[\frac{\omega_+ + \omega_-}{\left(\omega_+^2 + \gamma^2\right)\left(\omega_-^2 + \gamma^2\right)} - 2\frac{\lambda}{g}\frac{\omega_+\left(\omega_-^2 + \gamma^2\right)^2 + \omega_-\left(\omega_+^2 + \gamma^2\right)^2}{\left(\omega_+^2 + \gamma^2\right)^2\left(\omega_-^2 + \gamma^2\right)^2}\right]\tilde{b}e^{-i\omega_m t}, \qquad \text{(B6)}$$

$$\tilde{p} \approx -\frac{g\gamma\eta^2\left(\omega_+ + \omega_-\right)(A + iB)}{\left[\left(\omega_p - \omega_m\right)^2 + 4\gamma^2\right]\left(\omega_+^2 + \gamma^2\right)\left(\omega_-^2 + \gamma^2\right)}\tilde{b}, \qquad \text{(B7)}$$

with

$$A = 2\gamma\left\{1 - \frac{\lambda}{g}\left[1 + \frac{\omega_p^2\left(\omega_+\omega_- - \gamma^2\right)}{\left(\omega_+^2 + \gamma^2\right)\left(\omega_-^2 + \gamma^2\right)}\right] + \frac{\omega_p\left(\omega_p - \omega_m\right)}{4\gamma^2}\left[1 + \frac{\lambda}{g}\frac{\gamma^2\left(\omega_+^2 + \omega_-^2 + 3\gamma^2\right) - \omega_+^2\omega_-^2}{\left(\omega_+^2 + \gamma^2\right)\left(\omega_-^2 + \gamma^2\right)}\right]\right\}, \qquad \text{(B8)}$$

$$B = \omega_m\left[1 + \frac{\lambda}{g}\frac{\gamma^2\left(\omega_+^2 + \omega_-^2 + 3\gamma^2\right) - \omega_+^2\omega_-^2}{\left(\omega_+^2 + \gamma^2\right)\left(\omega_-^2 + \gamma^2\right)} + \frac{\lambda}{g}\frac{\omega_p - \omega_m}{\omega_m}\frac{2\gamma^2\left(\omega_+^2 + \omega_-^2 + 2\gamma^2\right) + \omega_p^2\left(\omega_+\omega_- - \gamma^2\right)}{\left(\omega_+^2 + \gamma^2\right)\left(\omega_-^2 + \gamma^2\right)}\right]. \qquad \text{(B9)}$$

Here, the second lines of Eqs. (B8) and (B9) vanish in the resonance case ($\omega_p = \omega_m$); these terms are only induced by the nonresonance situation ($\omega_p \neq \omega_m$). The terms $\propto \lambda/g$ in A [Eq. (B8)] and B [Eq. (B9)] are induced by the reconsidered optomechanical interaction. Because $A \propto \mathrm{Re}(\tilde{p})$ and $B \propto \mathrm{Im}(\tilde{p})$, from Eq. (B5), we know that A and B contribute to the frequency shift ω' and gain G of the phonon laser, respectively (see below).

Substitution of Eqs. (B6) and (B7) into the dynamical equation of $\tilde{b}$ in Eq. (B5) results in

$$\frac{d\tilde{b}}{dt} = \left(G - \gamma_m - i\omega'\right)\tilde{b}, \qquad \text{(B10)}$$

where

$$\omega' = \omega_0 + \omega_1 + \omega_2, \qquad \text{(B11)}$$

$$G = G_0 + G_1 + G_2. \qquad \text{(B12)}$$

Here, the frequency shift components ω_0, ω_1, and ω_2, and the laser gain components G_0, G_1, and G_2 are given by

$$\begin{aligned}\omega_0 &= \frac{g^2\Delta\hat{n}}{4\omega_m}\frac{\omega_p\left(\omega_p-\omega_m\right)+4\gamma^2}{\left(\omega_p-\omega_m\right)^2+4\gamma^2},\\ \omega_1 &= \frac{\lambda}{g}\left[\frac{\omega_m}{\Omega}\frac{\Omega\left(\omega_p-\omega_m\right)-\gamma f\ (3\gamma/\omega_m)}{\omega_p\left(\omega_p-\omega_m\right)+4\gamma^2}-2f\ (0)\right]\omega_0,\\ \omega_2 &= \frac{2\lambda^2}{g^2}\frac{\left(\omega_p-\omega_m\right)^2+4\gamma^2}{\omega_p\left(\omega_p-\omega_m\right)+4\gamma^2}\left[f\ \left(\frac{J}{\gamma}\right)+f\ (0)-1\right]\omega_0,\end{aligned} \tag{B13}$$

and

$$\begin{aligned}G_0 &= \frac{\gamma g^2\Delta\hat{n}}{2\left(\omega_p-\omega_m\right)^2+8\gamma^2},\\ G_1 &= \frac{\lambda}{g}\left[1-\frac{2\omega_p}{\omega_m}f\ \left(-\frac{\gamma}{\omega_p}\right)\right]G_0,\\ G_2 &= \frac{2\lambda}{g}\frac{\omega_p-\omega_m}{\omega_m}f\ \left(\frac{\omega_p}{4\gamma}\right)G_0,\end{aligned} \tag{B14}$$

with the photon number inversion $\Delta\hat{n}$, and the Fano-like spectrum profile $f\ (x)$, respectively:

$$\Delta\hat{n} = -\frac{4\Delta_L\omega_m\eta^2}{\gamma^2\omega_p^2\left(1+\Omega^2\right)}, \tag{B15}$$

$$f\ (x) = \frac{(x+\Omega)^2}{1+\Omega^2}-\frac{x^2}{1+\Omega^2}, \tag{B16}$$

where $\Omega = \left[\Delta_L^2-\left(\omega_p/2\right)^2+\gamma^2\right]/\left(\gamma\omega_p\right)$. Here, ω_0 and G_0 are the conventional frequency shift and laser gain (without the reconsidered optomechanical interaction), respectively, while ω_1, ω_2, G_1, and G_2 are, respectively, the frequency shifts and laser gains induced by the reconsidered optomechanical interaction. The frequency shifts ω_1 and ω_2 are related to the first order and the second order of λ/g, respectively. The gain G_1 is generally associated with the reconsidered optomechanical interaction, while G_2 is only present in the nonresonance case.

[1] R. M. Pettit, W. C. Ge, P. Kumar, D. R. Luntz-Martin, J. T. Schultz, L. P. Neukirch, M. Bhattacharya, and A. N. Vamivakas, An optical tweezer phonon laser, Nat. Photonics **13**, 402 (2019).

[2] J. B. Khurgin, Phonon lasers gain a sound foundation, Physics **3**, 16 (2010).

[3] S. Vashahri-Ghamsari, Q. Lin, B. He, and M. Xiao, Magnomechanical phonon laser beyond the steady state, Phys. Rev. A **104**, 033511 (2021).

[4] A. A. Geraci, S. B. Papp, and J. Kitching, Short-Range Force Detection Using Optically Cooled Levitated Microspheres, Phys. Rev. Lett. **105**, 101101 (2010).

[5] G. Ranjit, M. Cunningham, K. Casey, and A. A. Geraci, Zeptonewton force sensing with nanospheres in an optical lattice, Phys. Rev. A **93**, 053801 (2016).

[6] V. Braginsky, S. Strigin, and S. Vyatchanin, Parametric oscillatory instability in Fabry–Perot interferometer, Phys. Lett. A **287**, 331 (2001).

[7] M. R. Hush, W. B. Li, S. Genway, I. Lesanovsky, and A. D. Armour, Spin correlations as a probe of quantum synchronization in trapped-ion phonon lasers, Phys. Rev. A **91**, 061401(R) (2015).

[8] U. Kemiktarak, M. Durand, M. Metcalfe, and J. Lawall, Mode Competition and Anomalous Cooling in a Multimode Phonon Laser, Phys. Rev. Lett. **113**, 030802 (2014).

[9] J. B. Khurgin, M. W. Pruessner, T. H. Stievater, and W. S. Rabinovich, Laser-Rate-Equation Description of Optomechanical Oscillators, Phys. Rev. Lett. **108**, 223904 (2012).

[10] B. Peng, Ş. K. Özdemir, W. J. Chen, F. Nori, and L. Yang, What is and what is not electromagnetically induced transparency in whispering-gallery microcavities, Nat. Commun. **5**, 5082 (2014).

[11] Y. Chu, P. Kharel, W. H. Renninger, L. D. Burkhart, L. Frunzio, P. T. Rakich, and R. J. Schoelkopf, Quantum acoustics with superconducting qubits, Science **358**, 199 (2017).

[12] K. Vahala, M. Herrmann, S. Knünz, V. Batteiger, G. Saathoff, T. W. Hänsch, and Th. Udem, A phonon laser, Nat. Phys. **5**, 682 (2009).

[13] T. F. Kuang, R. Huang, W. Xiong, Y. L. Zuo, X. Han, F. Nori, C.-W. Qiu, H. Luo, H. Jing, and G. Z. Xiao, Nonlinear multi-frequency phonon lasers with active levitated optomechanics, Nat. Phys. **19**, 414 (2023).

[14] I. S. Grudinin, H. Lee, O. Painter, and K. J. Vahala, Phonon Laser Action in a Tunable Two-Level System, Phys. Rev. Lett. **104**, 083901 (2010).

[15] G. Z. Wang, M. M. Zhao, Y. C. Qin, Z. Q. Yin, X. S. Jiang, and M. Xiao, Demonstration of an ultra-low-threshold phonon laser with coupled microtoroid resonators in vacuum, Photonics Res. **5**, 73 (2017).

[16] J. Zhang, B. Peng, Ş. K. Özdemir, K. Pichler, D. O. Krimer, G. Zhao, F. Nori, Y.-X. Liu, S. Rotter, and L. Yang, A phonon laser operating at an exceptional point, Nat. Photonics **12**, 479 (2018).

[17] J. T. Mendonca, H. Tercas, G. Brodin, and M. Marklund, A phonon laser in ultra-cold matter, Europhys. Lett. **91**, 33001 (2010).

[18] A. Khaetskii, V. N. Golovach, X. Hu, and I. Žutić, Proposal for a Phonon Laser Utilizing Quantum-Dot Spin States, Phys. Rev. Lett. **111**, 186601 (2013).

[19] J. Kabuss, A. Carmele, T. Brandes, and A. Knorr, Optically Driven Quantum Dots as Source of Coherent Cavity Phonons: A Proposal for a Phonon Laser Scheme, Phys. Rev. Lett. **109**, 054301 (2012).

[20] I. Bargatin and M. L. Roukes, Nanomechanical Analog of a Laser: Amplification of Mechanical Oscillations by Stimulated Zeeman Transitions, Phys. Rev. Lett. **91**, 138302 (2003).

[21] I. Mahboob, K. Nishiguchi, A. Fujiwara, and H. Yamaguchi, Phonon Lasing in an Electromechanical Resonator, Phys. Rev. Lett. **110**, 127202 (2013).

[22] R. P. Beardsley, A. V. Akimov, M. Henini, and A. J. Kent, Coherent Terahertz Sound Amplification and Spectral Line Narrowing in a Stark Ladder Superlattice, Phys. Rev. Lett. **104**, 085501 (2010).

[23] M. Aspelmeyer, T. J. Kippenberg, and F. Marquardt, Cavity optomechanics, Rev. Mod. Phys. **86**, 1391 (2014).

[24] M. T. Hill, H. J. S. Dorren, T. de Vries, X. J. M. Leijtens, J. H. den Besten, B. Smalbrugge, Y.-S. Oei, H. Binsma, G.-D. Khoe, and M. K. Smit, A fast low-power optical memory based on coupled micro-ring lasers, Nature **432**, 206 (2004).

[25] F. N. Xia, L. Sekaric, and Y. Vlasov, Ultracompact optical buffers on a silicon chip, Nat. Photonics **1**, 65 (2007).

[26] F. Morichetti, C. Ferrari, A. Canciamilla, and A. Melloni, The first decade of coupled resonator optical waveguides: Bringing slow light to applications, Laser Photonics Rev. **6**, 74 (2012).

[27] L. Chang, X. S. Jiang, S. Y. Hua, C. Yang, J. M. Wen, L. Jiang, G. Y. Li, G. Z. Wang, and M. Xiao, Parity-time symmetry and variable optical isolation in active-passive-coupled microresonators, Nat. Photonics **8**, 524 (2014).

[28] B. Peng, Ş. K. Özdemir, F. C. Lei, F. Monifi, M. Gianfreda, G. L. Long, S. H. Fan, F. Nori, C. M. Bender, and L. Yang, Parity-time symmetric whispering-gallery microcavities, Nat. Phys. **10**, 394 (2014).

[29] L. Tang, J. S. Tang, M. Y. Chen, F. Nori, M. Xiao, and K. Y. Xia, Quantum Squeezing Induced Optical Nonreciprocity, Phys. Rev. Lett. **128**, 083604 (2022).

[30] C. Zheng, X. S. Jiang, S. Y. Hua, L. Chang, G. Y. Li, H. B. Fan, and M. Xiao, Controllable optical analog to electromagnetically induced transparency in coupled high-Q microtoroid cavities, Opt. Express **20**, 18319 (2012).

[31] S. V. Boriskina and L. D. Negro, Self-referenced photonic molecule bio(chemical) sensor, Opt. Lett. **35**, 2496 (2010).

[32] H. J. Kimble, The quantum internet, Nature **453**, 1023 (2008).

[33] A. Reiserer and G. Rempe, Cavity-based quantum networks with single atoms and optical photons, Rev. Mod. Phys. **87**, 1379 (2015).

[34] H. Wang, Z. X. Wang, J. Zhang, Ş. K. Özdemir, L. Yang, and Y.-X. Liu, Phonon amplification in two coupled cavities containing one mechanical resonator, Phys. Rev. A **90**, 053814 (2014).

[35] A. Metelmann and A. A. Clerk, Quantum-Limited Amplification via Reservoir Engineering, Phys. Rev. Lett. **112**, 133904 (2014).

[36] H. Jing, Ş. K. Özdemir, X. Y. Lü, J. Zhang, L. Yang, and F. Nori, $\mathcal{PT}$-Symmetric Phonon Laser, Phys. Rev. Lett. **113**, 053604 (2014).

[37] H. Lü, Ş. K. Özdemir, L.-M. Kuang, F. Nori, and H. Jing, Exceptional Points in Random-Defect Phonon Lasers, Phys. Rev. Appl. **8**, 044020 (2017).

[38] B. Peng, Ş. K. Özdemir, S. Rotter, H. Yilmaz, M. Liertzer, F. Monifi, C. M. Bender, F. Nori, and L. Yang, Loss-induced suppression and revival of lasing, Science **346**, 328 (2014).

[39] Y. Jiang, S. Maayani, T. Carmon, F. Nori, and H. Jing, Nonreciprocal Phonon Laser, Phys. Rev. Appl. **10**, 064037 (2018).

[40] B. He, L. Yang, and M. Xiao, Dynamical phonon laser in coupled active-passive microresonators, Phys. Rev. A **94**, 031802(R) (2016).

[41] Z. R. Gong, H. Ian, Y.-X. Liu, C. P. Sun, and F. Nori, Effective Hamiltonian approach to the Kerr nonlinearity in an optomechanical system, Phys. Rev. A **80**, 065801 (2009).

[42] R. Khan, F. Massel, and T. T. Heikkilä, Cross-Kerr nonlinearity in optomechanical systems, Phys. Rev. A **91**, 043822 (2015).

[43] N. Nishiguchi, S. Tamura, and Franco Nori, Phonon-transmission rate, fluctuations,and localization in random semiconductor superlattices: Green's-function approach, Phys. Rev. B **48**, 2515 (1993).

[44] J. Zhang, B. Peng, Ş. K. Özdemir, Y.-X. Liu, H. Jing, X.-Y Lü, Y.-L. Liu, L. Yang, and F. Nori, Giant nonlinearity via breaking parity-time symmetry: A route to low-threshold phonon diodes, Phys. Rev. B **92**, 115407 (2015).

[45] P. Rabl, Photon Blockade Effect in Optomechanical Systems, Phys. Rev. Lett. **107**, 063601 (2011).

[46] A. Nunnenkamp, K. Børkje, and S. M. Girvin, Single-Photon Optomechanics, Phys. Rev. Lett. **107**, 063602 (2011).

[47] J. Q. Liao and F. Nori, Photon blockade in quadratically coupled optomechanical systems, Phys. Rev. A **88**, 023853 (2013).

[48] R. Huang, A. Miranowicz, J.-Q. Liao, F. Nori, and H. Jing, Nonreciprocal Photon Blockade, Phys. Rev. Lett. **121**, 153601 (2018).

[49] R. Huang, Ş. K. Özdemir, J.-Q. Liao, F. Minganti, L.-M. Kuang, F. Nori, and H. Jing, Exceptional Photon Blockade: Engineering Photon Blockade with Chiral Exceptional Points, Laser Photonics Rev. **16**, 2270034 (2022).

[50] Y. L. Zuo, R. Huang, L.-M. Kuang, X.-W. Xu, and H. Jing, Loss-induced suppression, revival, and switch of photon blockade, Phys. Rev. A **106**, 043715 (2022).

[51] H. Xie, C. G. Liao, X. Shang, M. Y. Ye, and X. M. Lin, Phonon blockade in a quadratically coupled optomechanical system, Phys. Rev. A **96**, 013861 (2017).

[52] H. Xie, C. G. Liao, X. Shang, Z. H. Chen, and X. M. Lin, Optically induced phonon blockade in an optomechanical system with second-order nonlinearity, Phys. Rev. A **98**, 023819 (2018).

[53] L. L. Zheng, T. S. Yin, Q. Bin, X. Y. Lü, and Y. Wu, Single-photon-induced phonon blockade in a hybrid spin-optomechanical system, Phys. Rev. A **99**, 013804 (2019).

[54] T. C. H. Liew and V. Savona, Single Photons from Coupled Quantum Modes, Phys. Rev. Lett. **104**, 183601 (2010).

[55] M. Bamba, A. Imamoğlu, I. Carusotto, and C. Ciuti, Origin of strong photon antibunching in weakly nonlinear photonic molecules, Phys. Rev. A **83**, 021802(R) (2011).

[56] H. Flayac and V. Savona, Unconventional photon blockade, Phys. Rev. A **96**, 053810 (2017).

[57] B. J. Li, R. Huang, X. W. Xu, A. Miranowicz, and H. Jing, Nonreciprocal unconventional photon blockade in a spinning optomechanical system, Photonics Res. **7**, 630 (2019).

[58] M. Fleischhauer, A. Imamoglu, and J. P. Marangos, Electromagnetically induced transparency: Optics in coherent media, Rev. Mod. Phys. **77**, 633 (2005).

[59] K. J. Boller, A. Imamoglu, and S. E. Harris, Observation of Electromagnetically Induced Transparency, Phys. Rev. Lett. **66**, 2593 (1991).
[60] M. O. Scully, S. Y. Zhu, and A. Gavrielides, Degenerate Quantum-Beat Laser: Lasing Without Inversion and Inversion Without Lasing, Phys. Rev. Lett. **62**, 2813 (1989).
[61] S. E. Harris, Lasers Without Inversion: Interference of Lifetime-Broadened Resonances, Phys. Rev. Lett. **62**, 1033 (1989).
[62] U. Fano, Effects of configuration interaction on intensities and phase shifts, Phys. Rev. **124**, 1866 (1961).
[63] A. E. Miroshnichenko, S. Flach, and Y. S. Kivshar, Fano resonances in nanoscale structures, Rev. Mod. Phys. **82**, 2257 (2010).
[64] Y. H. Ahn, S. B. Choe, J. C. Woo, D. S. Kim, S. T. Cundiff, J. M. Shacklette, and Y. S. Lim, Quantum Interference of Virtual and Real Amplitudes in a Semiconductor Exciton System, Phys. Rev. Lett. **89**, 237403 (2002).
[65] B. Wang, H. Xiong, X. Jia, and Y. Wu, Phonon laser in the coupled vector cavity optomechanics, Sci. Rep. **8**, 282 (2018).
[66] Y. Dong, F. Bariani, and P. Meystre, Phonon Cooling by an Optomechanical Heat Pump, Phys. Rev. Lett. **115**, 223602 (2015).
[67] J. Guo, R. Norte, and S. Gröblacher, Feedback Cooling of a Room Temperature Mechanical Oscillator Close to Its Motional Ground State, Phys. Rev. Lett. **123**, 223602 (2019).
[68] C. Whittle, *et al.*, Approaching the motional ground state of a 10-kg object, Science **372**, 1333 (2021).
[69] Y. Seis, T. Capelle, E. Langman, S. Saarinen, E. Planz, and A. Schliesser, Ground state cooling of an ultracoherent electromechanical system, Nat. Commun. **13**, 1507 (2022).
[70] A. Schliesser, R. Riviere, G. Anetsberger, O. Arcizet, and T. J. Kippenberg, Resolved-sideband cooling of a micromechanical oscillator, Nat. Phys. **4**, 415 (2008).
[71] J. D. Teufel, T. Donner, D. Li, J. W. Harlow, M. S. Allman, K. Cicak, A. J. Sirois, J. D. Whittaker, K. M. Lehnert, and R. W. Simmonds, Sideband cooling of micromechanical motion to the quantum ground state, Nature **475**, 359 (2011).
[72] J. Chan, T. P. M. Alegre, A. H. Safavi-Naeini, J. T. Hill, A. Krause, S. Gröblacher, M. Aspelmeyer, and O. Painter, Laser cooling of a nanomechanical oscillator into its quantum ground state, Nature **478**, 89 (2011).
[73] S. Kotler, G. A. Peterson, E. Shojaee, F. Lecocq, K. Cicak, A. Kwiatkowski, S. Geller, S. Glancy, E. Knill, R. W. Simmonds, J. Aumentado, and J. D. Teufel, Direct observation of deterministic macroscopic entanglement, Science **372**, 622 (2021).
[74] L. M. de Lépinay, C. F. Ockeloen-Korppi, M. J. Woolley, and M. A. Sillanpää, Quantum mechanics–free subsystem with mechanical oscillators, Science **372**, 625 (2021).
[75] S. Knünz, M. Herrmann, V. Batteiger, G. Saathoff, T. W. Hänsch, K. Vahala, and Th. Udem, Injection Locking of a Trapped-Ion Phonon Laser, Phys. Rev. Lett. **105**, 013004 (2010).
[76] Z. C. Liu, Y. Q.Wei, L. Chen, J. Li, S. Q. Dai, F. Zhou, and M. Feng, Phonon-Laser Ultrasensitive Force Sensor, Phys. Rev. Appl. **16**, 044007 (2021).
[77] Y. Q. Wei, Y. Z. Wang, Z. C. Liu, T. H. Cui, L. Chen, J. Li, S. Q. Dai, F. Zhou, and M. Feng, Detection of DC electric forces with zeptonewton sensitivity by single-ion phonon laser, Sci. China Phys. Mech. Astron. **65**, 110313 (2022).
[78] T. Behrle, T. L. Nguyen, F. Reiter, D. Baur, B. de Neeve, M. Stadler, M. Marinelli, F. Lancellotti, S. F. Yelin, and J. P. Home, A phonon laser in the quantum regime, ArXiv:2301.08156.
[79] B. Wang, Z.-X. Liu, X. Jia, H. Xiong, and Y. Wu, Polarization-based control of phonon laser action in a parity time-symmetric optomechanical system, Commun. Phys. **1**, 43 (2018).
[80] R. Huang and H. Jing, The nanosphere phonon laser, Nat. Photonics **13**, 372 (2019).
[81] J. Kabuss, A. Carmele, and A. Knorr, Threshold behavior and operating regimes of an optically driven phonon laser: Semiclassical theory, Phys. Rev. B **88**, 064305 (2013).
[82] A. Dunn, C. Poyser, P. Dean, A. Demić, A. Valavanis, D. Indjin, M. Salih, I. Kundu, L. H. Li, A. Akimov, A. G. Davies, E. Linfield, J. Cunningham, and A. Kent, High-speed modulation of a terahertz quantum cascade laser by coherent acoustic phonon pulses, Nat. Commun. **11**, 835 (2020).
[83] N. Lörch and K. Hammerer, Sub-Poissonian phonon lasing in three-mode optomechanics, Phys. Rev. A **91**, 061803(R) (2015).